ELSEVIER

PII: S0011-2275(98)00060-5

Cryogenics **38** (1998) 911–915

Printed in Great Britain
0011-2275/98/$—see front matter

Point contact tunnelling apparatus with temperature and magnetic field control

L. Ozyuzer*†‡, J.F. Zasadzinski†‡ and K.E. Gray†

†Science and Technology Center for Superconductivity, Argonne National Laboratory, Argonne, IL 60439, USA
‡Illinois Institute of Technology, Chicago, IL 60616, USA

Received 1 December 1997

The design and testing of a new device for point contact tunnelling measurements in superconductors are described. The insert is designed for use with a continuous flow cryostat which allows for a large range of sample temperatures from 1.5 K to room temperature. The use of nonmagnetic parts allows tunnelling measurements to be performed in high magnetic fields. Testing was carried out on a conventional superconductor, Nb, in fields up to 6 T using Nb and Au tips to obtain superconductor–insulator–superconductor and superconductor–insulator–normal metal junctions. In addition, a moderate-T_c oxide superconductor, $Ba_{1-x}K_xBiO_3$, was used to obtain temperature and magnetic field dependencies of the energy gap.

Keywords: tunnelling spectroscopy; superconductors; cryostat

Tunnelling spectroscopy is a powerful tool for studying the superconducting density of states (DOS) near the Fermi energy level[1]. It also gives sensitive information about the electronic interaction spectrum (e.g. electron–phonon in Pb), and in a few cases even the symmetry of the energy gap in conventional and high-T_c superconductors (HTS). The superconducting DOS at $T = 0$ K is obtained[2] from the ratio of the tunnelling conductance in the superconducting state (σ_s) to the tunnelling conductance in the normal state (σ_n). While σ_s is readily measured at $T \ll T_c$, the measurement of σ_n can be difficult. One approach is to introduce a magnetic field to quench the superconductivity. Another approach is to raise the temperature to a value above T_c, and the large H_{c2} for optimally doped HTS[3] makes the latter approach more convenient. In addition, the temperature dependence of the tunnelling conductance can give important information on the energy gap, $\Delta(T)$, and provides a local measurement of T_c. Features above T_c such as pseudogaps in HTS can also be explored with a wide range of temperature control. Point contact tunnelling (PCT) has proved to be an extremely valuable tool for tunnelling into HTS materials. However, a measurement over the wide temperature range of HTS is difficult because of thermal expansions in the PCT apparatus, e.g., between the tip and sample. The junction may be altered, or lost as the temperature is varied.

To accomplish the above goals, a new high-field apparatus with significantly improved temperature control was built and is described here. It is based on our previous tunnelling apparatus, described elsewhere[4], which was shown to accurately reproduce the quasiparticle DOS observed in planar junctions of Nb, including the subtle phonon structure which represents a deviation of about 1% in the conductance[5]. Previous PCT system designs have been reported[6,7], including one for use in high magnetic fields, but they are not capable of carrying out normal state conductance of high temperature superconductors. This report presents the design and operation of a new cryostat insert which allows for point contact tunnelling measurements in high magnetic field and varying temperatures. To the best of our knowledge, this is the widest temperature range and lowest noise tunnelling system which has been made that incorporates mechanical junctions. The insert can also be extended to operate as an STM.

Theoretical background

The tunnel current in superconductor–insulator–superconductor (S–I–S) and superconductor–insulator–normal metal (S–I–N) junctions can be written as[2]

$$I(V) = c \int_{-\infty}^{\infty} |T|^2 \rho_1(E)\rho_2(E + eV)[f(E) - f(E + eV)]\mathrm{d}E \qquad (1)$$

Here, $\rho_1(E)$ and $\rho_2(E)$ are the quasiparticle DOS in the two electrodes, c is a proportionality constant, $f(E)$ is the

*To whom correspondence should be addressed.

Fermi–Dirac distribution function which describes thermal smearing, and $|T|^2$ is the tunnelling matrix element. If $|T|^2$ varies slowly for the voltage range of the experiment ($eV \leq 2\Delta$), the tunnelling matrix element may be assumed to be energy independent and taken out of the integral. For an S–I–N junction where electrode 1 is a normal metal, $\rho_1(E) = 1$, and in the limit $T = 0$ K, the tunnelling conductance, $\sigma_s = dI/dV$ becomes

$$\sigma_s(V) = c|T|^2\rho_2(E) = \sigma_n(V)\rho(E) \qquad (2)$$

where we have now assumed $E = eV$. The superconducting density of states for a BCS superconductor is given by

$$\rho(E) = \frac{|E|}{\sqrt{E^2 - \Delta^2}} \quad |E| \geq \Delta$$
$$= 0 \quad |E| < \Delta$$

where Δ is the energy gap. An exact determination of $\rho(E)$ requires a measurement of normal state (background) conductance $\sigma_n(V)$ to divide out the unknown prefactors of Equation (2).

Added complications accompany HTS. It is difficult to justify the assumption that $|T|^2$ is independent of energy over the wide range needed to explore the HTS gap, Δ. Typically $2\Delta \sim 70$ meV, which is not small compared to a barrier height of say 300 meV. Furthermore, the two-dimensional band structure of HTS may have important effects on the tunnelling DOS. This might lead to an additional momentum dependence to $|T|^2$. In some cases the background conductance has a strong voltage dependence, as seen in $Bi_2Sr_2CaCu_2O_{8+x}$[8]. In the PCT and STM studies, asymmetric and decreasing background shapes are usually obtained, including a relatively strong dip in the occupied states of the band. It is crucial to understand which, if any, of these effects are intrinsic to the HTS or due to tunnelling matrix element effects. As a result, accurate background measurements are needed for a correct interpretation of the data.

As we mentioned before, to obtain σ_n, one approach is to apply a magnetic field to suppress the superconductivity. However, in the case of optimally doped HTS, the upper critical field (H_{c2}) can be very high[3] and is usually beyond the capability of most systems. On the other hand, with sufficient over- or underdoping of HTS, T_c may decrease enough to lower H_{c2} into an accessible range of magnetic fields. For this to work, a high field capability is needed.

Insert design

The continuous flow cryostat[9] is a versatile apparatus which allows measurements over a wide temperature range (1.5–300 K). A magnet installed on such systems can produce fields up to 19 T. In continuous flow cryostats, cryogens (liquid helium or nitrogen) flow from the main reservoir through a capillary tube to the sample chamber, which is isolated from the cryogen reservoir. The rate of flow of the cryogen can be regulated to control the sample temperature (*Figure 1*). The sample temperature can be changed by: (A) varying the flow rate of the cryogen through the needle valve; (B) using the heat exchanger/vaporizer at the bottom of the sample tube; or (C) pumping on the sample region to produce evaporative cooling. A temperature sensor, placed near to the vaporizer, can be used for monitoring and providing a feedback loop to regulate the temperature at a set value using a current output to the vaporizer (*Figure 1*). Coarse temperature control for PCT measurements is discussed below. Gas flow cryostats allow the sample to be changed without removing helium from the He reservoir, which saves time and operation cost.

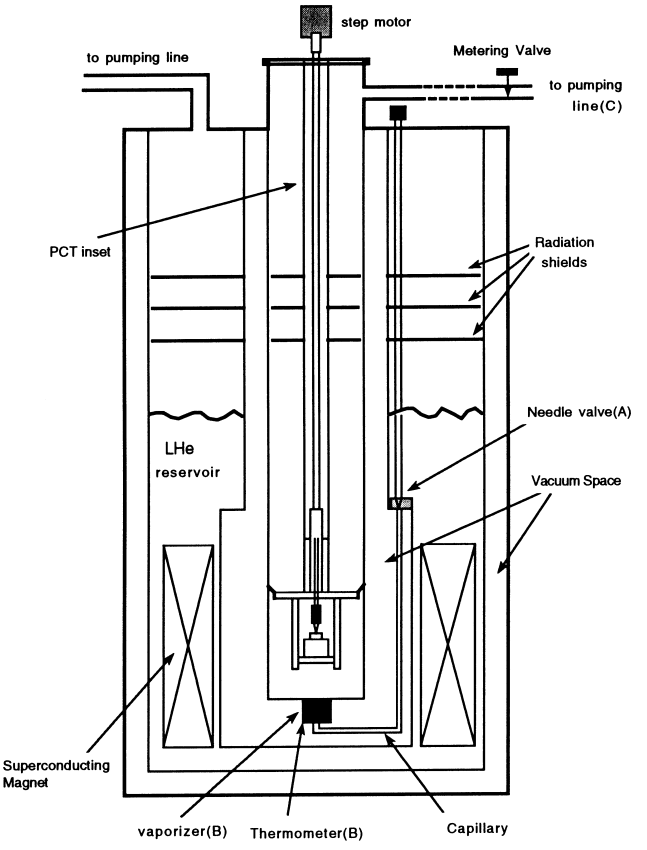

Figure 1 Schematic representation of continuous flow cryostat

There were three important factors that were taken into account in the design and operation of the PCT insert described herein. They are broad magnetic field and temperature variation capabilities, design against electrical, acoustical and vibrational noise, and ease of use, which includes a compatibility with commercial cryostats.

Since a large magnetic field will be applied to the bottom part of the insert which contains the sample and tip assembly, it is essential that the material used in the construction be nonmagnetic over a substantial portion of the 6 T range. Therefore, the differential micrometer, which is attached to the tip and the sample cage, has been made of titanium, which has a lower magnetic permeability than stainless steel (machining stainless steel makes it magnetic). In addition, titanium has a lower thermal expansion coefficient than stainless steel, which minimizes the effect of relative thermal expansion between sample and tip, and partly compensates the relative displacements during temperature variations. *Figure 2* shows the bottom part of the insert. The coarse approach of the sample to the tip along the *z*-direction is made by the plate A on which the sample is mounted. A commercial micropositioner[10] (B and C) has been used for coarse adjustment in *x–y* plane before placing the insert into the cryostat. This micropositioner is important to adjust the *x–y* position of the specimen under the tip, and is necessary with extremely small crystals. We have successfully performed tunnelling measurements of

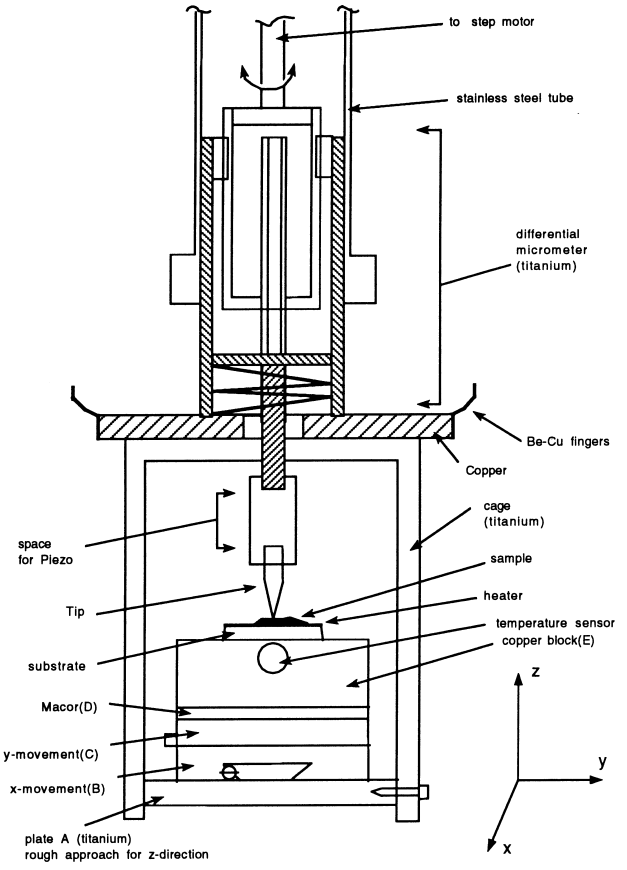

Figure 2 Schematic representation of the bottom part of the insert

single crystal specimens as small as (0.5 mm × 0.5 mm). There is a copper block (E) which is thermally isolated with Macor layer (D) on the micropositioner, and it has a hole for a temperature sensor which is close to where the sample is placed. Temperature has been probed by a Cernox temperature sensor [11], which has an extremely small magnetoresistance. A heater is placed between the sample and copper block and connected to a temperature controller. The *z* (vertical) position of the tunnelling tip is controlled by a differential micrometer which has a total travel of 0.4 mm and a *z* displacement 11.5 nm per degree of revolution. For PCT, absolute vertical height of the tip is not important, because the tip is in contact with the sample. A stainless steel tube holds the differential micrometer. Inside this tube there is another stainless steel tube which drives the micrometer for fine adjustment. There is a decoupling between the micrometer and this tube to prevent vibrations that may come from the flange. The tube is driven by a small electric motor which is placed out of the flange on top of the insert. The cage has only three small windows to allow adjustment of the sample and shields the tip from the direct cooling of the He gas which comes from the vaporizer.

The quality of information extracted from PCT measurements is improved by acoustic and electric shielding and by suppressing thermal fluctuations. In addition, the tunnel junctions between sample and tip will be formed by mechanical contact, so this mechanical system has to be stable against external (ground) and internal (gas flow) vibrations to obtain an acceptable signal-to-noise ratio. The system is housed inside of a complete electrically and acoustically screened room located in a quiet corner of a laboratory basement. The small, rigid design of the tip assembly is most sensitive to high vibrational frequencies, and good decoupling is necessary to eliminate such vibrations. The helium dewar holding the apparatus is supported above the floor by three air suspension legs[12] to decouple it from low-frequency ground vibrations. Approximately 500 kg of lead bricks are piled uniformly around the perimeter of the upper plate of the platform top to lower the resonant frequency and to improve the damping of any oscillations of the air table. The cryostat sits inside a silica sand-filled plastic drum on the lower plate of the platform. Fine silica sand isolates the sample region from acoustical noise. There is another silica sand box to isolate vibration which comes from outside via cables and rubber vacuum hose. All these precautions allow a stable junction to be maintained during the data acquisition.

The various ways to change the temperature of the sample have been mentioned above. For mechanical stability of the junction, it has been found that adjusting the gas-flow needle valve is not acceptable for coarse temperature variation after a particular junction is formed, because it requires direct contact with the cryostat. The metering valve is preferred, because it is mechanically isolated from the cryostat with a rubber hose and a sand box. The vaporizer and sample heater are connected to LakeShore 91C temperature controllers[11] to fine control the temperature to within an accuracy of 0.01 K between 1.5 K and 300 K. The magnetic field is obtained using a 6 T superconducting magnet and controlled with a typical stability of 1 mT.

A sweep circuit is used to supply current and two preamplifiers are used to simultaneously measure I and V of the junction. The high-input-impedance, differential preamplifiers isolate the junction from the x–y recorder and data acquisition system. While the tip is pushed against the crystal the $I(V)$ signal is continuously monitored using an oscilloscope until an acceptable junction is obtained. The quality of the junction can be judged using the criteria of low zero bias conductance and high conductance peak at the gap voltage. First derivative measurements were obtained using a bridge with the usual lock-in procedure[2]. Data are saved on a computer and plotted on a chart simultaneously.

Performance of the system

The system has been tested using a well-known conventional superconductor, high-purity Nb foil, and a moderate-T_c superconductor $Ba_{1-x}K_xBiO_3$. Tips of both Nb and Au were cleaned with diamond paper before each low-temperature run. The tips and Nb foil were etched (in aqua regia for Au and HF for Nb tip and foil) then mounted on the sample holder. *Figure 3* shows the current–voltage characteristics of four different S–I–S (in this case Nb tip–Insulator–Nb foil) junctions at 4.2 K. Junction resistances range from 4 kΩ to 85 kΩ. The ohmic behavior of the I–V curves at high bias is expected in conventional superconductors. While the nature of the barrier is not known for certain, it is likely due to the insulating Nb_2O_5 which forms on air-exposed Nb surfaces. The reduced area of the PCT junction (contact diameter ~ 2400 Å)[5] and the ability to move point-to-point enhances the probability of finding a tunnel junction that is free of barrier defects.

The best way to measure the energy gap of a superconductor utilizes S–I–S junctions at $T \ll T_c$, since quasiparti-

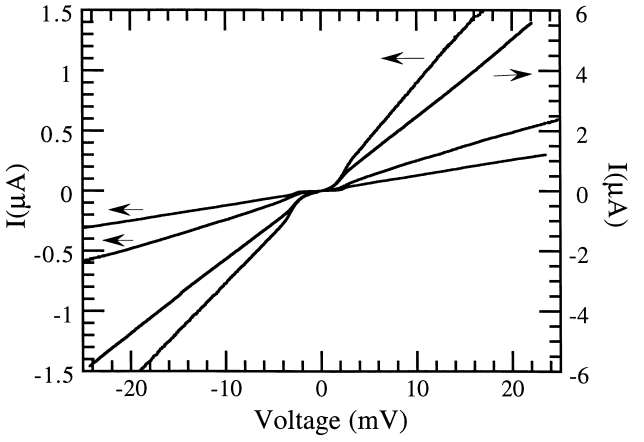

Figure 3 Current–voltage characteristics of four different S–I–S (Nb tip–Insulator–Nb foil) junctions at 4.2 K

cle peak positions are not affected by thermal smearing or other broadening mechanisms. In addition, conductance peaks are very sharp relative to S–I–N junctions. *Figure 4* shows the normalized conductance of an S–I–S junction at 4.2 K (full circles). Data are analyzed using Equation (1) plus a phenomenological smearing parameter Γ, such that

$$\rho(E) = \mathrm{Re}\left\{ \frac{E - i\Gamma}{\sqrt{(E - i\Gamma)^2 - \Delta^2}} \right\}$$

and the fit (solid line) results in $\Delta(T = 4.2\ \mathrm{K}) = 1.5$ meV and $\Gamma = 0.2$ meV. In the context of BCS approximation, $\Delta(0) = 1.54$ meV is obtained which is in excellent agreement with previous published data[13]. In this case, the flat background leaves no doubt about the normalized conductance. It is obtained by dividing the conductance by a constant value. The inset in *Figure 4* shows expanded Nb sample/Au tip conductances at 4.2 K. The upper conductance curve is regenerated from Huang *et al.*[5], which was taken in our earlier PCT system. In the lower curve, the data are taken in the present system and clear phonon structures can be seen in both curves.

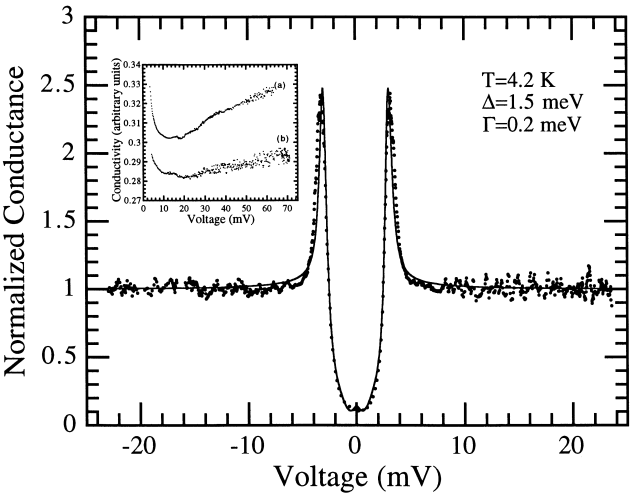

Figure 4 Normalized conductance versus voltage characteristics of S–I–S junction at 4.2 K (full circles). Solid line represents a numerical fit which corresponds to convolution of the BCS DOS at 4.2 K. For the BCS DOS, the energy gap parameters are $\Delta = 1.5$ meV and $\Gamma = 0.2$ meV. The inset shows the expanded scale of conductivity in the region of phonon structure for Nb foil/Au tip junction. (a) Huang *et al.*[5], (b) present work

The disadvantage of testing the system with a conventional superconductor is that a flat background is obtained very often. Furthermore the low T_c does not test the limits of our system. We have therefore extended the above testing of the system to include $Ba_{1-x}K_xBiO_3$, which is an oxide superconductor similar to HTS cuprates, with T_c varying with K doping from 20 to 32 K. So it is a perfect candidate for this study.

Samples of $Ba_{1-x}K_xBiO_3$ (nominally with $x = 0.375$) were prepared from the oxide powders (Bi_2O_3, BaO and KO_2) in a melt-process technique described previously[14]. Tunnelling results on these polycrystals have been published earlier[15]. Here, we reproduced those results and measured the temperature and magnetic field dependence of the same samples to test the system. Because of the aging effects, the surface color has changed from deep blue to black. Magnetic susceptibility measurements indicate that T_c degraded to 28 K. The surface of the samples was polished with various grades of diamond paper, the final one with 3 μm diameter grit size paper. The samples were then blown clean with dry N_2 gas, after contacts were applied. Temperatures below 4.2 K are obtained filling the sample chamber with liquid He, closing the needle valve and reducing the pressure by a vacuum pump. *Figure 5* shows an S–I–N junction conductance for $Ba_{1-x}K_xBiO_3$ at 1.5 K. The voltage, *V*, is that of the tip relative to the sample. This means that negative bias region corresponds to occupied states in the DOS. The curve displays low (almost zero) zero bias conductance, flat subgap feature, well-resolved quasiparticle peaks and phonon structure which fulfill requirements of high-quality tunnelling data.

Figure 6 shows dynamic conductances of an S–I–N junction at different temperatures. For $T > T_c$, the figure explicitly shows that the background is not flat and exhibits an asymmetric, weakly increasing behavior. Now, to obtain the normalized conductance, the $T = 29$ K curve conductance can be used. Normalized conductance has been found $\sigma = \sigma(T = 4.2\ \mathrm{K})/\sigma(T = 29\ \mathrm{K})$, and fitted to the BCS DOS (including lifetime smearing) resulting in an energy gap value of 4.2 meV. Because the main purpose of this paper is to prove the reliability of the design, more detailed discussions of $Ba_{1-x}K_xBiO_3$ data are deferred to a future article.

We have also examined the magnetic field dependence

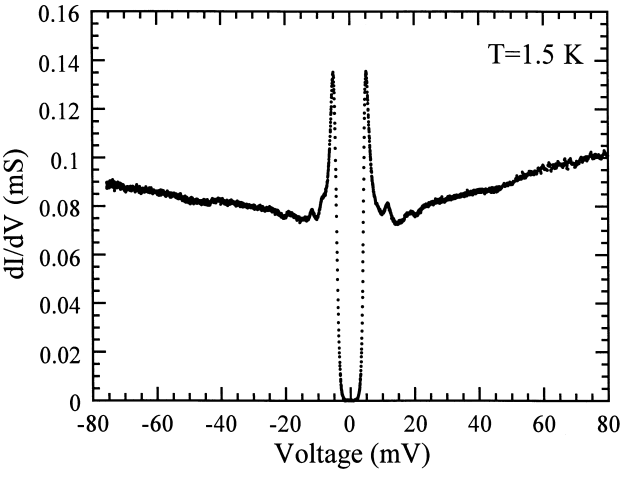

Figure 5 S–I–N tunnelling conductance of $Ba_{1-x}K_xBiO_3$ at 1.5 K

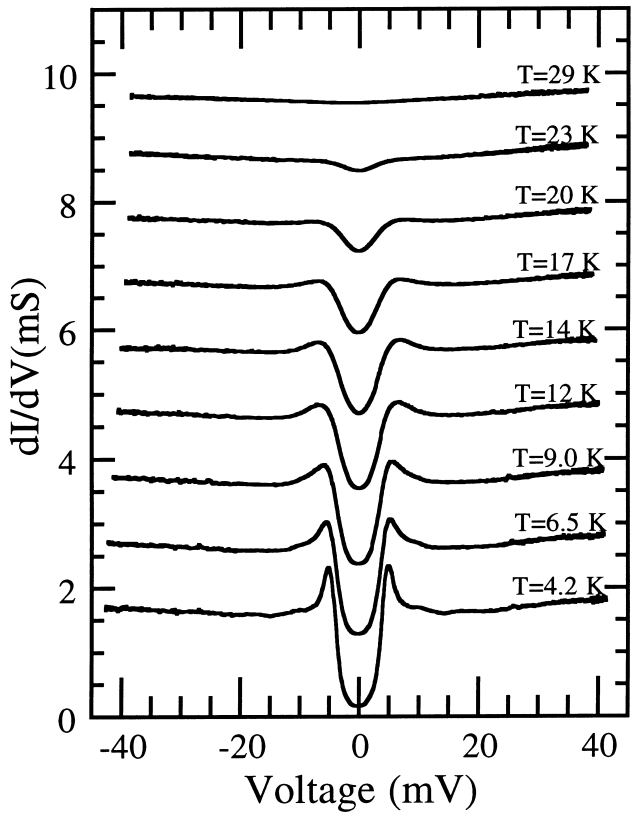

Figure 6 Dynamic conductance of $Ba_{1-x}K_xBiO_3$ for different temperatures. Data have been shifted vertically by 1σ, 2σ, ..., for clarity (σ = 1.0 mS). T = 29 K curve corresponds to normal state conductance

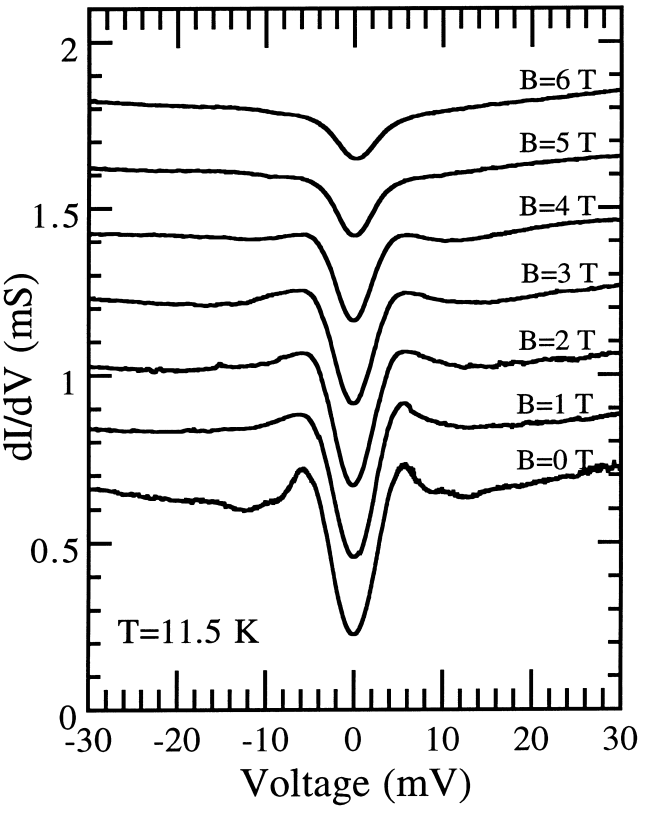

Figure 7 Magnetic field behavior of dynamic conductance of $Ba_{1-x}K_xBiO_3$ at 11.5 K. Data have been shifted vertically by 1σ,2σ, ..., for clarity (σ = 0.2 mS). Superconductivity exists even at 6 T

of S–I–N (Au tip) junction at 11.5 K, as seen in *Figure 7*. Applying magnetic fields up to 6 T does not completely suppress superconductivity in $Ba_{1-x}K_xBiO_3$. The quasiparticle peak height gradually decreases and the zero bias conductance increases. Based on the phase diagram of $Ba_{1-x}K_xBiO_3$, from Klein *et al.*[16], a magnetic field greater than 20 T is needed to obtain normal state conductance at 11.5 K.

In summary, we have designed and tested a new insert for point-contact tunnelling measurements. We have demonstrated that the system is very reliable and versatile for tunnelling studies of superconductors. Even at this early stage of development, the system has reproduced some of our best data obtained at 4.2 K in comparison with our earlier design. In addition, we have demonstrated a wide range of temperature and magnetic field control. Future work will involve HTS cuprates, with an explicit attempt to measure $\Delta(T)$ and to study in detail the origin of the unusual background features found in the tunnelling conductances.

Acknowledgements

This work was partially supported by the US Department of Energy, Division of Basic Energy Sciences–Material Sciences under contract No. W-31-109-ENG-38, and the National Science Foundation, Office of Science and Technology Centers under contract No. DMR 91-20000. LO acknowledges support from Izmir Institute of Technology, Turkey. The authors would like to thank Zikri Yusof for valuable discussions.

References

1. Hasegawa, T., Ikuta, H. and Kitazawa, K., *Physical Properties of High Temperature Superconductors III*, ed. D. M. Ginsberg. World Scientific, Singapore, 1993.
2. Wolf, E. L., *Principles of Electron Tunneling Spectroscopy*. Oxford University Press, New York, 1985.
3. Tsuda, N., Nasu, K., Yanase, A. and Siratori, K., *Electronic Conduction in Oxides*. Springer, Berlin, 1991.
4. Hawley, M. E., Gray, K. E., Terris, B. D., Wang, H. H., Carlson, K. D. and Williams, J. M., *Phys. Rev. Lett.*, 1986, **57**, 629.
5. Huang, Q., Zasadzinski, J. F. and Gray, K. E., *Phys. Rev. B*, 1990, **42**, 7953.
6. Srikanth, H. and Raychaudhuri, A. K., *Cryogenics*, 1991, **31**, 421.
7. Shivashankar, G. V. and Rajeev, K. P., *Meas. Sci. Technol.*, 1991, **2**, 1031.
8. Zasadzinski, J. F., Ozyuzer, L., Yusof, Z., Chen, J., Gray, K. E., Mogilevsky, R., Hinks, D. G., Cobb, J. L. and Markert, J. T., *Spectroscopic Studies of High T_c Cuprates*, Vol. 2696, ed. I. Bozovic and D. van der Marel. Proc. SPIE, Bellingham, p. 338.
9. Janis Research Company, Wilmington, MA 01887.
10. Charles Supper Co. Inc., Natick, MA 01760.
11. Lake Shore Cryotronics, Inc. Westerville, OH 43081.
12. Pneumatic isolation mounts type XLC, Newport Corporation, Fountain Valley, CA 92728.
13. Khim, Z. G., Burnell, D. M. and Wolf, E. L., *Solid State Commun.*, 1981, **39**, 159.
14. Hinks, D. G., Mitchell, A. W., Zang, Y., Richards, D. R. and Dabrowski, B., *Appl. Phys. Lett.*, 1989, **54**, 1585.
15. Huang, Q., Zasadzinski, J. F., Tralshawala, N., Gray, K. E., Hinks, D. G., Peng, J. L. and Greene, R. L., *Nature* (London), 1990, **347**, 369; Huang, Q., Zasadzinski, J. F., Gray, K. E., Richards, D. R. and Hinks, D. G., *Appl. Phys. Lett.*, 1990, **57**, 22.
16. Klein, T., Baril, L., Escribe-Filippini, C., Marcus, J. and Jansen, A. G. M., *Phys. Rev. B*, 1996, **53**, 9337.